Clinical Cancer Research

T-Cell Exhaustion Signatures Vary with Tumor Type and Are Severe in Glioblastoma

Karolina Woroniecka[1,2], Pakawat Chongsathidkiet[1,2], Kristen Rhodin[1], Hanna Kemeny[1], Cosette Dechant[1], S. Harrison Farber[1], Aladine A. Elsamadicy[1], Xiuyu Cui[1], Shohei Koyama[3], Christina Jackson[4], Landon J. Hansen[5], Tanner M. Johanns[6], Luis Sanchez-Perez[1], Vidyalakshmi Chandramohan[7], Yen-Rei Andrea Yu[8], Darell D. Bigner[7], Amber Giles[9], Patrick Healy[10], Glenn Dranoff[3], Kent J. Weinhold[11], Gavin P. Dunn[12], and Peter E. Fecci[1,2]

Abstract

Purpose: T-cell dysfunction is a hallmark of glioblastoma (GBM). Although anergy and tolerance have been well characterized, T-cell exhaustion remains relatively unexplored. Exhaustion, characterized in part by the upregulation of multiple immune checkpoints, is a known contributor to failures amid immune checkpoint blockade, a strategy that has lacked success thus far in GBM. This study is among the first to examine, and credential as *bona fide*, exhaustion among T cells infiltrating human and murine GBM.

Experimental Design: Tumor-infiltrating and peripheral blood lymphocytes (TILs and PBLs) were isolated from patients with GBM. Levels of exhaustion-associated inhibitory receptors and poststimulation levels of the cytokines IFNγ, TNFα, and IL2 were assessed by flow cytometry. T-cell receptor Vβ chain expansion was also assessed in TILs and PBLs. Similar analysis was extended to TILs isolated from intracranial and subcutaneous immunocompetent murine models of glioma, breast, lung, and melanoma cancers.

Results: Our data reveal that GBM elicits a particularly severe T-cell exhaustion signature among infiltrating T cells characterized by: (1) prominent upregulation of multiple immune checkpoints; (2) stereotyped T-cell transcriptional programs matching classical virus-induced exhaustion; and (3) notable T-cell hyporesponsiveness in tumor-specific T cells. Exhaustion signatures differ predictably with tumor identity, but remain stable across manipulated tumor locations.

Conclusions: Distinct cancers possess similarly distinct mechanisms for exhausting T cells. The poor TIL function and severe exhaustion observed in GBM highlight the need to better understand this tumor-imposed mode of T-cell dysfunction in order to formulate effective immunotherapeutic strategies targeting GBM. *Clin Cancer Res; 24(17); 4175–86. ©2018 AACR.*

See related commentary by Jackson and Lim, p. 4059

Introduction

Glioblastoma (GBM) is the most common and feared malignant primary brain tumor, persisting as one of few cancers that remain universally lethal. Despite improvements in standard of care, median survival remains at just 15 to 17 months (1). Immunotherapies continue to yield promise, but the efficacy needed to garner an FDA approval has remained wanting. Success has been limited by marked tumor heterogeneity (2), poor immune infiltration (3), and the tumor's notably potent capacities for subverting local and systemic immune responses. Regarding the latter, it is the T cells required for effective antitumor responses that are particularly victimized (4–6). Their plight is reflected in patient lymphopenia (7), as well as various characterized forms of classical T-cell dysfunction, such as anergy (8, 9) and regulatory T-cell–imposed tolerance (10–13). Countering such dysfunction has not yet reliably yielded sustained and effective T-cell activity within the tumor, however, raising concerns for additional unexplored tumor-imposed states of T-cell dysfunction, such as exhaustion. Despite sporadic studies suggesting T-cell phenotypes that might signal exhaustion, few formal characterizations of T-cell exhaustion in patients or mice with GBM have been undertaken.

T-cell exhaustion is a hyporesponsive state resulting from repeated or prolonged antigenic exposure under suboptimal conditions (14). Initially discovered in the context of chronic lymphocytic choriomeningitis virus (LCMV) infection (14, 15), it is now known to contribute to disrupted T-cell function in cancer as well (16). Exhaustion represents a specific transcriptional program in T cells that is often characterized

[1]Duke Brain Tumor Immunotherapy Program, Department of Neurosurgery, Duke University Medical Center, Durham, North Carolina. [2]Department of Pathology, Duke University Medical Center, Durham, North Carolina. [3]Department of Medical Oncology and Cancer Vaccine Center, Dana Farber Cancer Institute, Boston, Massachusetts. [4]Department of Neurosurgery, Johns Hopkins University, Baltimore, Maryland. [5]Department of Pharmacology and Molecular Cancer Biology, Duke University, Durham, North Carolina. [6]Division of Medical Oncology, Department of Medicine, Washington University, St. Louis, Missouri. [7]Department of Neurosurgery, Duke University Medical Center, Durham, North Carolina. [8]Department of Medicine, Duke University Medical Center, Durham, North Carolina. [9]Neuro-oncology Division, National Institutes of Health, Bethesda, Maryland. [10]Department of Biostatistics, Duke University, Durham, North Carolina. [11]Department of Surgery, Duke University Medical Center, Durham, North Carolina. [12]Department of Neurological Surgery, Center for Human Immunology and Immunotherapy Programs, Washington University, St. Louis, Missouri.

Note: Supplementary data for this article are available at Clinical Cancer Research Online (http://clincancerres.aacrjournals.org/).

Corresponding Author: Peter E. Fecci, Duke University Medical Center, Box 3050, Durham, NC 27705. Phone: 919-681-1010; Fax: 919-684-9045; E-mail: peter.fecci@duke.edu

doi: 10.1158/1078-0432.CCR-17-1846

Translational Relevance

Primary malignant brain neoplasms are responsible for over 15,000 deaths annually in the United States. Although several immunotherapeutic strategies have shown remarkable success and are FDA approved in other malignancies, immunotherapies for glioblastoma (GBM) have shown limited success in clinical trials. Immunotherapies are potentially limited in GBM by several factors, including tumor heterogeneity, low tumor mutational burden, low levels of T-cell infiltration, and GBM's potent immunosuppressive capabilities. The latter most prominently results in profound T-cell dysfunction, damaging the efficacy of immune-based platforms. Much of the immunotherapeutic focus has been on activating T cells and ensuring their access to tumors situated within the confines of the brain. We demonstrate, however, that those T cells successfully arriving at the tumor are still rendered hyporesponsive by the tumor, with exhaustion revealed as a significant mode of dysfunction. Notably, we find that GBM elicits a particularly severe exhaustion signature among infiltrating T cells, characterized by prominent upregulation of multiple immune checkpoints and stereotyped exhaustion transcriptional signatures. The severity of the observed T-cell exhaustion suggests tumor-imposed dysfunction that might not be reversed with immune checkpoint blockade alone, highlighting the new and urgent need to address the underlying mechanisms contributing to tumor-imposed exhaustion in order to formulate effective immunotherapies targeting GBM.

phenotypically by the increased expression of multiple coinhibitory receptors, many of which constitute classical or alternative immune checkpoints (17). Known receptors include PD-1, CTLA-4, TIM-3, LAG-3, BTLA, 2B4, CD160, CD39, VISTA, and TIGIT. Antagonizing or blocking PD-1 and CTLA-4 (the classical immune checkpoints) are well-recognized FDA-approved anticancer strategies aimed at improving T-cell function in multiple malignancies, including melanoma and non–small cell lung carcinoma. To date, such strategies have shown only limited efficacy in GBM, creating the need to better understand treatment failures. One mechanism conferring resistance to classical checkpoint blockade has been the upregulation of alternative immune checkpoints such as TIM-3 and LAG-3 (18), signifying that T-cell exhaustion might play a substantial role in restraining therapeutic enhancements to T-cell function in GBM. To date, few thorough investigations of classical and alternative immune checkpoint coexpression within GBM have been conducted. Likewise, the prominence of exhaustion among tumor-infiltrating lymphocytes (TILs) and its contribution to local T-cell dysfunction in GBM are poorly described.

We report here that a substantial proportion of TILs derived from human GBM express multiple coinhibitory immune checkpoints. These findings are recapitulated in two different murine models of glioma, where the mounting expression of PD-1, Tim-3, and Lag-3 correspond to diminished TIL responsiveness. TILs from glioma demonstrate significant dysfunction, and their transcriptional signatures and epigenetic profiles match that of traditional *bona fide* T-cell exhaustion, as described in viral models. Interestingly, in our murine tumor models, patterns of TIL exhaustion prove to be tumor type-specific, with gliomas, lung carcinoma, breast carcinoma, and melanoma all eliciting characteristic, yet distinct exhaustion signatures that do not vary when tumor site is modified, including when each tumor is placed intracranially. Likewise, independent of location, the exhaustion signature and corresponding TIL dysfunction appear to be particularly severe among T cells infiltrating gliomas, highlighting a significant contribution for exhaustion to T-cell dysfunction within these tumors.

Materials and Methods

Patient samples

All studies were conducted with approval from the Massachusetts General Hospital Cancer Center Institutional Review Board or the Duke Cancer Center Institutional Review Board. All studies were conducted in accordance with recognized ethical guidelines (U.S. Common Rule, 45 CFR 46, 21 CFR 50, 21 CFR 56, 21 CFR 312, 21 CFR 812, and 45 CFR 164.508-514) 21 treatment-naïve GBM patients undergoing primary surgical resection of intracranial (i.c.) GBM were included in the prospective collection of whole blood and tumor tissue. Fifteen healthy age-matched controls were included in the prospective collection of whole blood. Informed consent was obtained from all subjects. Blood specimens were collected into EDTA-containing tubes. All blood and tumor specimens were stored at room temperature and processed within 12 hours. All samples were labeled directly with antibodies for use in flow cytometry, and red blood cells subsequently lysed using eBioscience RBC lysis buffer (eBioscience). Cells were washed, fixed, and analyzed on an LSRII FORTESSA flow cytometer (BD Bioscience).

Mice

Female C57BL/6 and VM-Dk mice were used at 6 to 12 weeks of age. C57BL/6 mice were purchased from Charles River Laboratories. VM-Dk mice were bred and maintained as a colony at Duke University. Animals were maintained under specific pathogen-free conditions at Cancer Center Isolation Facility of Duke University Medical Center. The Institutional Animal Care and Use Committee approved all experimental procedures.

Cell lines

Cell lines studied included SMA-560 malignant glioma, CT2A malignant glioma, E0771 breast medullary adenocarcinoma, B16F10 melanoma, and Lewis Lung Carcinoma (LLC). SMA-560 cells are syngeneic on the VM-Dk background, whereas all others are syngeneic in C57BL/6 mice. The SMA-560 cell line is derived from a spontaneous malignant glioma that originally arose on the VM-Dk background. Tumors have low S-100 expression and high glial fibrillary acid protein expression, and are most representative of anaplastic astrocytoma (19). The CT2A cell line is derived from a chemically induced tumor with 20-methylcholanthrene on the C57BL/6 background, and accurately reflects several characteristics of GBM including intratumoral heterogeneity, as well as radio- and chemoresistance (20). SMA-560, CT2A, B16F10, and LLC cells were grown *in vitro* in DMEM with 2 mmol/L L-glutamine and 4.5 mg/mL glucose (Gibco) containing 10% FBS (Gemini Bio-Products). E0771 cells were grown *in vitro* in RPMI 1640 (Gibco) containing

10% FBS plus 1% HEPES (Gibco). Cells were harvested in the logarithmic growth phase. For i.c. implantation, tumor cells in PBS were then mixed 1:1 with 3% methylcellulose and loaded into a 250 μL syringe (Hamilton). The needle was positioned 2 mm to the right of the bregma and 4 mm below the surface of the skull at the coronal suture using a stereotactic frame. Note that 1×10^4 SMA-560, CT2A, E0771, and LLC cells or 500 B16F10 cells were delivered in a total volume of 5 μL per mouse. For s.c. implantation, 5×10^5 SMA-560, CT2A, E0771, and LLC cells or 2.5×10^5 B16F10 cells were delivered in a total volume of 200 μL per mouse into the s.c. tissues of the left flank.

Tissue processing

Tumors were minced, incubated in 100 units/mL collagenase IV (Sigma-Aldrich) and 0.1 mg/mL DNase I (Roche Diagnostics) in RPMI supplemented with 10% FBS for 20 to 30 minutes in a Stomacher machine set at normal speed, and washed through 70-μm nylon cell strainers (Falcon; BD Biosciences) in PBS with 2% FBS. Cells were immediately stained and subsequently analyzed by flow cytometry.

Flow cytometry and cytokine detection

Human-specific antibodies were purchased from BD Biosciences (CD3: SP34-2; CD4: RPA-T4) or BioLegend (CD8: HIT8a; PD1: EH12.2H7; TIM-3: F38-2E2; LAG3-: 11C3C65; CTLA-4: BNI3; TIGIT: A15153G; CD39: A1; IL2: MQ1-17H12; TNFα: MAb11; IFNγ: 4S.B3. Mouse-specific antibodies were purchased from BD Biosciences (CD3: 145-2C11; CD4: RM4-5; CD8: 53-6.7; PD1: J43; Lag-3: C9B7W; TIGIT: 1G9; CD244.2: 2B4; CD160: CNX46-3; CTLA4: UC10-4F10) or Biolegend (IFNγ: XMG1.2; IL2: JES6-5H4; TNFα: MP6-XT22; Tim-3: RMT3-23; CD39: Duha59; BTLA: 8F4). Appropriate isotype controls were used when applicable. The LIVE/DEAD Fixable Yellow Dead Cell Stain Kit (Thermo Fisher) was used to exclude dead cells. Intracellular staining was performed using the eBioscience Fixation and Permeabilization Buffer kit. For intracellular cytokine staining, cells were stimulated with phorbol 12-myristate 13-acetate (PMA, 50 nmol/L) and ionomycin (500 nmol/L) for 4 to 6 hours at 37°C, 5% CO_2, in the presence of 1 μg/mL brefeldin A (BD biosciences). Surface staining was performed, and cells were fixed and permeabilized with the BD Cytofix/Cytoperm Kit and stained for IFNγ, TNFα, and IL2. Tetramers for mODC1 were generated and used as described previously (21).

Analysis of T-cell receptor Vβ repertoire

Five patient TILs and peripheral blood mononuclear cells (PBMCs) and five control PBMCs were isolated as described above. The repertoire was assessed using the IOTest Beta Mark TCR V beta Repertoire Kit (Cat: IM3497 Beckman Coulter) according to the manufacturer's instructions.

Gene expression analysis

When moribund, tumor-bearing animals were sacrificed and T cells were isolated and sorted from tumors and spleens based on the following markers: Live, $CD45^+$, $CD3^+$, $CD8^+$. $CD8^+$ T cells isolated from tumor-draining (TD) cervical lymph nodes (LNs) were additionally stained and sorted for $CD44^+$. RNA was extracted using the Qiagen RNAeasy Mini Kit (Cat No: 74104) and DNase treated using Qiagen RNase-Free DNase Set (Cat No: 79254). RNA concentration and purity were determined with NanoDrop and RNA integrity with Agilent Bioanalyzer. cDNA was synthesized and hybridized to the Affymetrix Clariom S Mouse Array.

PD-1 methylation analysis

Genomic DNA was isolated from sorted $CD8^+$ T cells (as described previously) from tumors, spleens, or TD cervical LNs using the Quick-DNA Universal Kit (Cat No: D4068; Zymo Research) according to the manufacturer's instructions, and <1 μg of DNA was subjected to bisulfite conversion using the EZ DNA Methylation Kit (Cat No: D5001; Zymo Research). The bisulfite-converted DNA was then amplified for pyrosequencing analysis using the PyroMark PCR Kit (Qiagen; Cat No: 978703). Primers were selected for the CR-B site covering four CpG sites at the PD-1 promoter region as previously published (22). Pyrosequencing was performed on amplified bisulfite-converted DNA using PyroMark Gold Q96 Reagent (Qiagen; Cat No: 972807).

Statistical analysis

For human studies, the sample size of 21 patients and 10 controls was chosen so that a two-tailed *t* test comparing groups has 90% power to detect a difference that is 1.1 times the standard deviation of the outcome variable in each group. For animal studies, sample sizes were chosen based on historic experience and were variable based on numbers of surviving mice available at experimental timepoints or technical limitations. For statistical comparisons, unpaired *t* tests were generally used to compare groups. Analyses were not adjusted for multiple testing.

Results

T-cell–infiltrating human GBM expresses multiple immune checkpoints and exhibits impaired function

The checkpoint molecules PD-1, CTLA-4, TIM-3, LAG-3, CD160, 2B4, TIGIT, CD39, and BTLA have been identified as coinhibitory regulators of T-cell effector function during chronic viral infection and within tumors, limiting the scope and duration of T-cell responses (17, 23). Furthermore, their expression on T cells can frequently signal an exhausted state. To begin examining the contribution of exhaustion to T-cell dysfunction in GBM, we used flow cytometry to phenotypically analyze TILs and PBMCs isolated from treatment-naïve patients with GBM enrolled in a specimen collection protocol. PBMCs from healthy controls were isolated for comparison. Twenty-one patients were enrolled in total (patient and control characteristics listed in Supplementary Table S1).

We found that PD-1, LAG-3, TIGIT, and CD39, in particular, were highly expressed on patient $CD8^+$ TILs (Fig. 1A and B; gating strategy depicted in Supplementary Fig. S1A). Notably, PD-1 was especially prominent, being found on up to 96% of tumor-infiltrating $CD8^+$ T cells, with most of these in turn being PD-1^{hi}. Although the percentage of TIM-3^+ $CD8^+$ T cells was not statistically significantly greater among TILs than patient or control PBMCs ($P = 0.059$), TIM-3 was present on >20% of TILs in several patients, and the median fluorescence intensity (MFI) of TIM-3 was significantly greater on TILs than in control blood (Supplementary Fig. S1B). The majority of immune checkpoints studied were present to a greater extent among TILs than among either patient or control PBMCs. An exception was BTLA, which was lower among TILs, consistent with studies showing that BTLA is more highly expressed on naïve T cells and becomes downregulated following antigenic exposure (24). Regarding peripheral

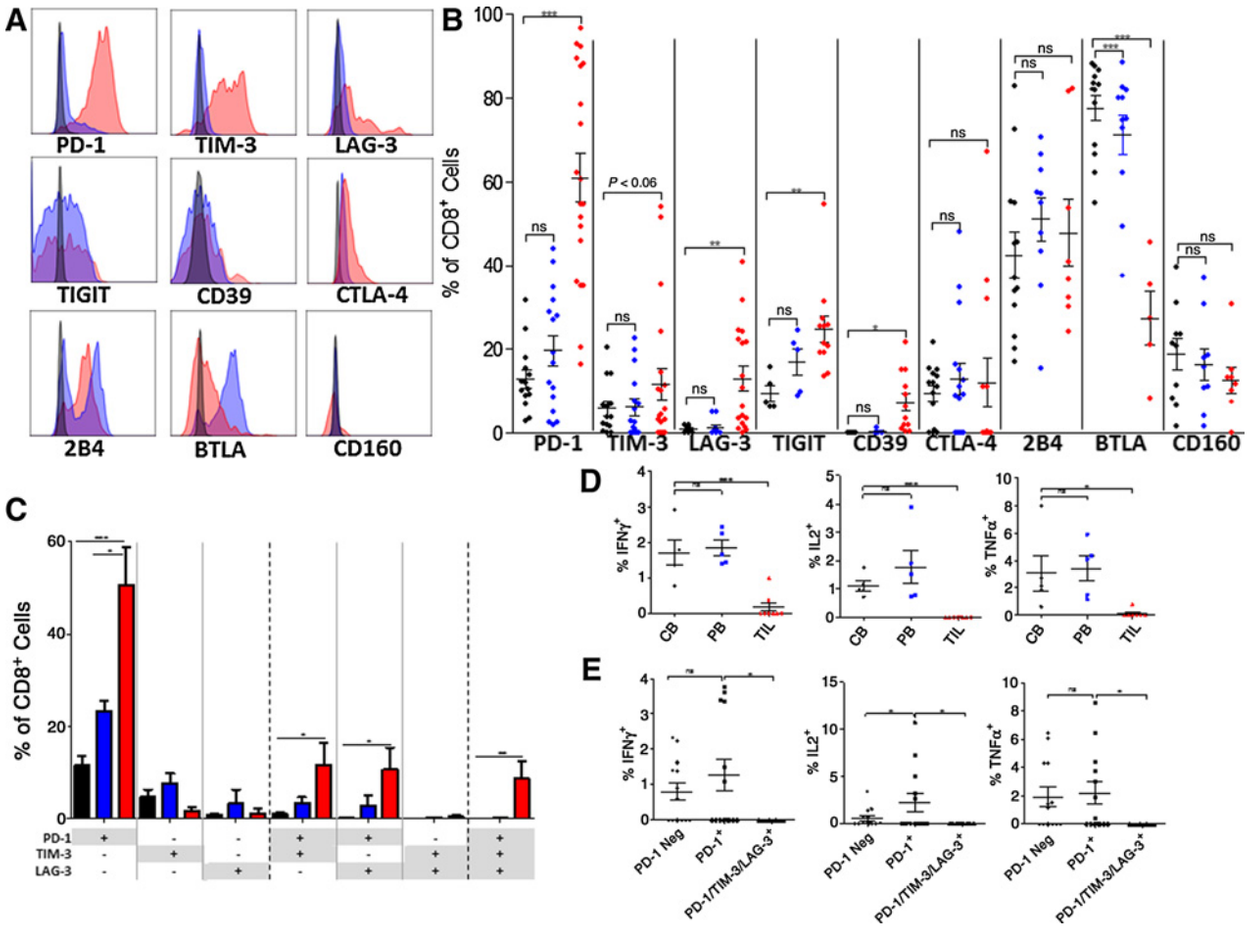

Figure 1.

Elevated expression of checkpoint molecules and decreased cytokine production among TILs in human GBM. **A,** Representative histograms of checkpoint molecule expression on CD8$^+$ T cells where red represents patient TILs, blue represents patient blood, and black represents relevant isotype control. CTLA-4 is an intracellular stain. **B,** Frequency of checkpoint molecule expression on CD8$^+$ T cells isolated from TILs (PD-1, TIM-3 $n = 20$; LAG-3 $n = 18$; CTLA-4 $n = 13$; CD39, TIGIT $n = 12$; CD160, 2B4 $n = 8$; BTLA $n = 5$), patient blood (PD-1, TIM-3 $n = 16$; CTLA-4 $n = 15$; 2B4, BTLA $n = 11$; LAG-3 $n = 12$; CD160 $n = 9$; TIGIT, CD39 $n = 5$), or control blood (PD-1, TIM-3, CTLA-4 $n = 14$; LAG-3 $n = 10$; 2B4, BTLA $n = 13$; CD160 $n = 10$; TIGIT, CD39 $n = 5$). **C,** Boolean gating was performed on CD8$^+$ T cells isolated from control and patient blood and patient tumors to determine coexpression of PD-1, TIM-3, and LAG-3. Sample numbers: control blood ($n = 9$), patient blood ($n = 6$), and patient TILs ($n = 5$). Bar graphs represent mean ± SEM. **D,** Poststimulation with PMA/Ionomycin intracellular staining was performed on patient TILs, blood, and control blood for IFNγ, IL2, and TNFα. **E,** Boolean gating was employed to determine percentage of cells producing cytokines among T cells not expressing PD-1, PD-1 single positive, or PD-1/TIM-3/LAG-3 triple positive cells. **B–D,** Red represents patient TILs, blue represents patient blood, and black represents control blood. Throughout figure *, $P < 0.05$; **, $P < 0.01$; and ***, $P < 0.0001$ by unpaired t test between control and patient samples.

blood, patient and control PBMCs did not differ substantially from each other with respect to checkpoint expression.

There was no difference in the percentage of CD8$^+$ T cells expressing 2B4, CD160, or CTLA-4 across tissue types or between patients and controls. MFI data for all checkpoint molecules are available in Supplementary Fig. S1B. Upon further characterization of T cells infiltrating human GBM, we found that tumor-infiltrating CD8$^+$ T cells demonstrated a predominantly effector memory T-cell phenotype (CD45RA$^-$CD62L$^-$) as opposed to naïve (CD45RA$^+$CD62L$^+$; Supplementary Fig. S2), reflecting prior antigenic exposure.

Although high levels of PD-1 expression on effector memory T cells can signal either activation or exhaustion, the mounting expression of additional alternative immune checkpoints frequently reflects the hierarchical loss of effector function, favoring the presence of T-cell exhaustion (17). Therefore, we evaluated the degree of coexpression between PD-1 and the common alternative immune checkpoints TIM-3 and LAG-3 on CD8$^+$ T cells from both tumors and blood. Boolean gating was employed to analyze the following T-cell populations: CD8$^+$ T cells that were positive for only one marker (e.g., PD-1$^+$TIM-3$^-$LAG-3$^-$), positive for two markers (e.g., PD-1$^+$TIM-3$^+$LAG-3$^-$), or triply positive (PD-1$^+$TIM-3$^+$LAG-3$^+$). Higher percentages of CD8$^+$ TILs in human GBM expressed either PD-1 alone, PD-1 in combination with TIM-3 or LAG-3, or all three markers, in comparison with CD8$^+$ T cells isolated from either patient or control blood (Fig. 1C). Single expression of TIM-3 or LAG-3 was not common in either TILs or blood. These findings reveal that both TIM-3 and

LAG-3 expressions are almost universally accompanied by PD-1 expression (and frequently by one another as well), with such coexpression suggesting a dysfunctional state.

We next assessed cytokine production of TILs and PBMCs to determine whether the high immune checkpoint expression in TILs predicted T-cell hyporesponsiveness. Following stimulation with PMA and ionomycin, intracellular IFNγ, IL2, and TNFα were assessed by flow cytometry. There was no difference in cytokine production between patient and control PBMCs, whereas TILs produced significantly less IFNγ, IL2, and TNFα than control PBMCs (Fig. 1D). Within patient samples, cells that were PD-1 negative or PD-1 single positive produced comparable amounts of IFNγ and TNFα, whereas cells that were PD-1 single positive produced more IL2 than PD-1–negative cells (Fig. 1E), highlighting that high levels of PD-1 alone may represent a state of activation rather than exhaustion. Mounting expression of the alterative immune checkpoints TIM-3 and LAG-3 resulted in loss of function: triply positive PD-1^{+}TIM-3^{+}LAG-3^{+} T cells were unable to produce IFNγ, IL2, or TNFα (Fig. 1E).

Multiple immune checkpoint expression on TILs is recapitulated in murine models of malignant glioma

To examine the degree to which these findings might be recapitulated in mice, we employed two common immunologically relevant orthotopic models of murine malignant glioma: SMA-560 and CT2A. Beginning with the CT2A model, we found that PD-1 was expressed by up to 95% of CD8^{+} TILs (Fig. 2A), similar to human GBM TILs. Tim-3, Lag-3, CTLA-4, 2B4, CD160, CD39, and TIGIT expressions were also notably prevalent and appeared to be more common than among GBM patient TILs, although no statistical comparisons across species were made.

CT2A TILs isolated from SMA-560 tumors likewise demonstrated increased expression of multiple immune checkpoints (particularly PD-1, Tim-3, Lag-3, and CD39), but consistently demonstrated less prominent upregulation of CTLA-4, 2B4, CD160, and TIGIT than what was found for CT2A (Fig. 2A and B). Both the CT2A and SMA-560 models demonstrated a substantial proportion of TILs that were triply positive for PD-1, Tim-3, and Lag-3: upon Boolean analysis, a mean of 40% and

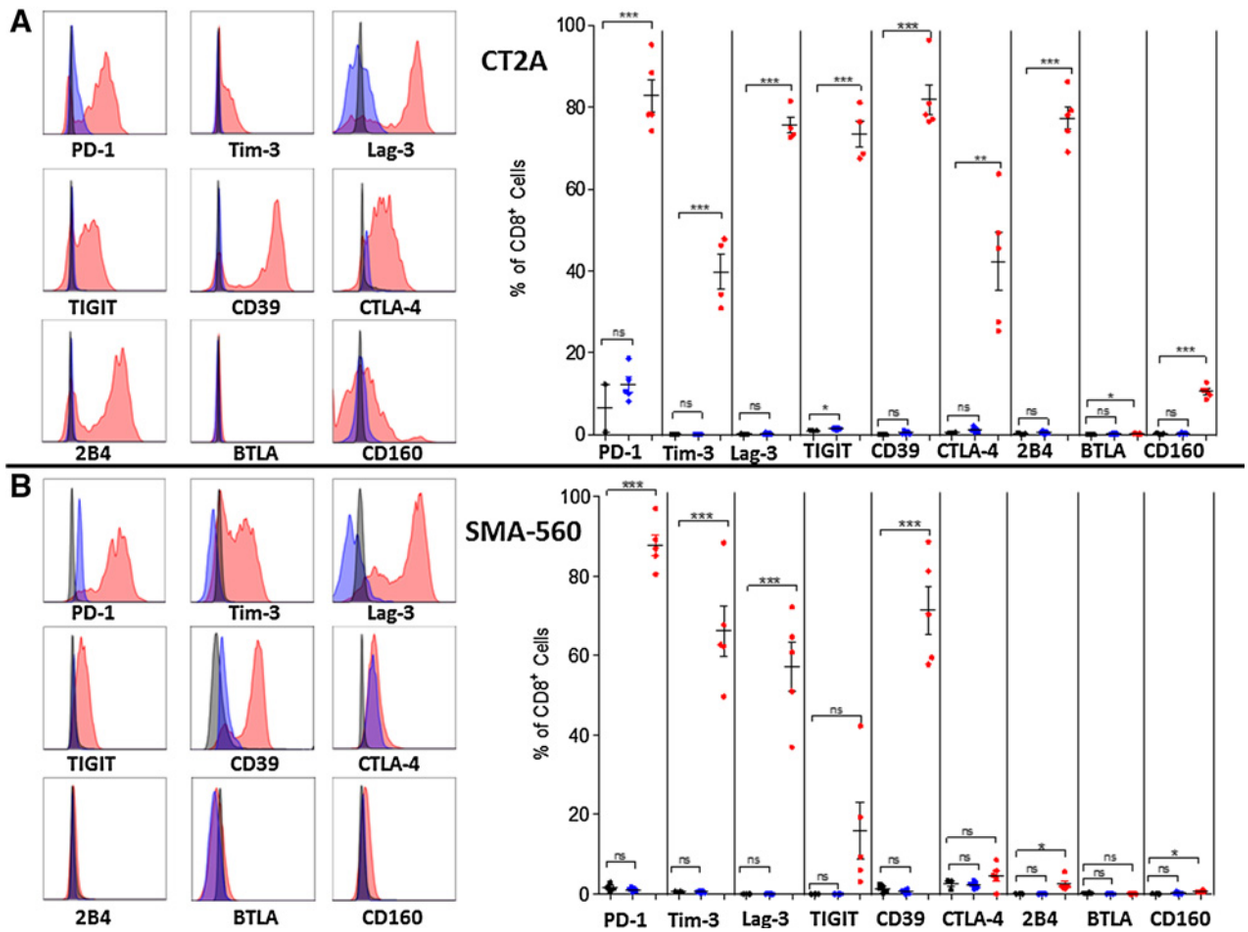

Figure 2.

Expression of multiple checkpoint molecules among TILs in CT2A and SMA-560 murine glioma models. Tumors and blood were harvested when mice were moribund at day 21 after i.c. tumor implantation ($n = 5$) for CT2A (**A**) or SMA-560 (**B**) tumor models. Representative histograms of checkpoint molecule expression on CD8^{+} T cells are shown where red represents TILs, blue represents tumor-bearing blood, and black represents relevant isotype control. For graphs, red represents TIL, blue represents tumor-bearing blood, and black represents naïve blood. Significance was determined using unpaired *t* test between control and tumor-bearing samples. *, $P < 0.05$; ***, $P < 0.001$.

46% of infiltrating CD8$^+$ T cells in CT2A and SMA-560, respectively, expressed all three immune checkpoints (Supplementary Fig. S3). Similarly, in both murine models, we found that PD-1 was expressed on the majority of CD8$^+$ TILs, whereas Tim-3 and Lag-3 were coexpressed with PD-1 rather than present on their own, akin to the observation in human GBM specimens.

TIL dysfunction, transcriptional signatures, and epigenetic modifications are consistent with *bona fide* T-cell exhaustion

To determine whether glioma TILs demonstrate decreased functional capacity compared with lymphocytes isolated from other compartments in tumor-bearing and naïve animals, we harvested lymphocytes from spleens, TD cervical LNs, and tumors at day 18 following i.c. implantation with CT2A. Lymphocytes were also harvested from spleens and LNs of age-matched naïve animals. As might be anticipated, CD8$^+$ TILs expressed greater numbers and levels of immune checkpoints than CD8$^+$ lymphocytes isolated from spleens or TDLNs (Fig. 3A). Notably, neither spleens nor LNs from tumor-bearing animals demonstrated appreciable differences in the percentages of single-positive PD-1, Tim-3, or Lag-3–expressing T cells when compared with the same lymphoid organs from naïve animals, further revealing such expression patterns as concentrated among TILs. Accompanying the phenotypic variations across TILs, spleen, and LNs, however, were significant differences in T-cell function across the compartments. Following stimulation with PMA and ionomycin, intracellular IFNγ, IL2, and TNFα were assessed by flow cytometry. Significantly fewer TILs were positive for IFNγ, IL2, and TNFα than lymphocytes isolated from either spleens or LNs, signaling a hyporesponsive state among TILs (Fig. 3B). The MFIs of IFNγ, IL2, and TNFα were also significantly lower among TILs than among T cells from other lymphoid compartments (Supplementary Fig. S4A). Representative dot plots are shown in Supplementary Fig. S4B. CD8$^+$ TIL staining positively for IFNγ, IL2, or TNFα were not uncommonly found to be PD-1 single positive (consistent with PD-1's ambiguous identity as an activation marker). TILs

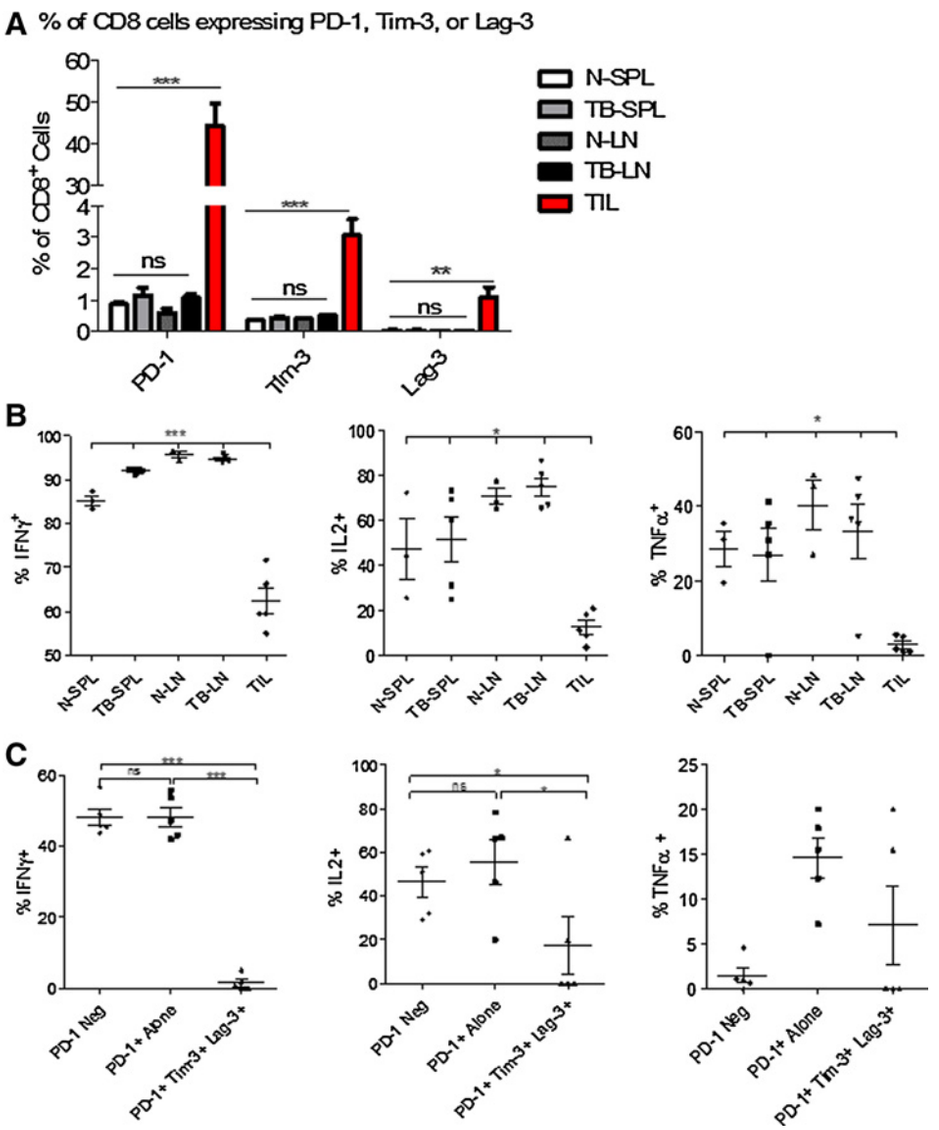

Figure 3.

TILs isolated from murine gliomas demonstrate impaired function. **A,** The percentage of CD8$^+$ T cells expressing either PD-1, Tim-3, or Lag-3 alone was compared across immunologic compartments. T cells were isolated from the spleens (SPL) and cervical LNs from either CT2A tumor-bearing (TB) ($n = 5$) or -naïve (N) ($n = 3$) mice, as well as from tumors of TB mice (TILs). **B,** The capacity for CD8$^+$ T cells isolated from the same sites to express IFNγ, IL2, and TNFα, upon stimulation with PMA/ionomycin, was compared. **C,** Boolean gating was employed to determine percentage of cells producing cytokines among TILs not expressing PD-1, PD-1 single positive, or PD-1/TIM-3/LAG-3 triple positive cells. Statistical significance was assessed via unpaired *t* test between control- and tumor-bearing samples. *, $P < 0.05$; **, $P < 0.01$; and ***, $P < 0.0001$ throughout the figure.

triply positive for PD-1, Tim-3, and Lag-3 produced significantly less IL2 than PD-1 singly positive TILs, and triply positive TILs trended toward decreased TNFα production, although a significant difference was not seen. T cells producing IFNγ were not found among triply positive TILs, indicating that mounting expression of alternative immune checkpoints corresponded to worsening function, particularly with regard to IFNγ and IL2 production (Fig. 3C).

To further assess glioma TILs for features of *bona fide* T-cell exhaustion, as described in models of chronic viral infection, we compared the gene-expression profiles of $CD8^+$ CT2A TILs with those of naïve ($CD44^-$) $CD8^+$ T cells isolated from spleens, or to activated ($CD44^+$) $CD8^+$ T cells isolated from TDLNs using the murine Clariom S microarray transcriptome-level platform (Affymetrix). The gene-expression profile of TILs differed significantly from the profile of either naïve or effector T cells (Fig. 4A). To determine whether this molecular signature was consistent with T-cell exhaustion, we used gene set enrichment analysis to compare the transcriptional profile of CT2A TILs with previously identified gene sets from virus-specific exhausted $CD8^+$ T cells isolated from chronic LCMV clone 13 infections (25). We found enrichment for exhaustion genes and pathways in CT2A TILs that statistically matched patterns observed in virally induced exhaustion (Fig. 4B).

T-cell exhaustion during chronic viral infection is associated with the loss of $Tbet^{hi}PD\text{-}1^{int}$ T cells, and the accumulation of terminally differentiated $Eomes^{hi}PD\text{-}1^{hi}$ exhausted T cells (26). Likewise, our data show that GBM TILs demonstrate elevated Eomes and decreased Tbet levels (Fig. 4C). Blimp-1, a transcription factor associated with T-cell exhaustion in chronic viral infections (27), is also elevated among CT2A TILs. As additional confirmation, we examined the methylation status of the PD-1 (pdcd1) gene locus. Chronic viral infection has been shown to enforce demethylation of the PD-1 locus in antigen-specific T cells (28). We found that the PD-1 locus is significantly demethylated in glioma TILs compared with naïve and effector T cells, consistent with expectations for T-cell exhaustion (Fig. 4D).

T-cell exhaustion arises preferentially amid tumor-specific T cells

To determine whether T-cell exhaustion arises moreso amid tumor-specific T cells, we utilized the SMA-560 glioma model. The SMA-560 glioma model expresses the recently characterized ODC1-Q129L mutation, which results in a functionally

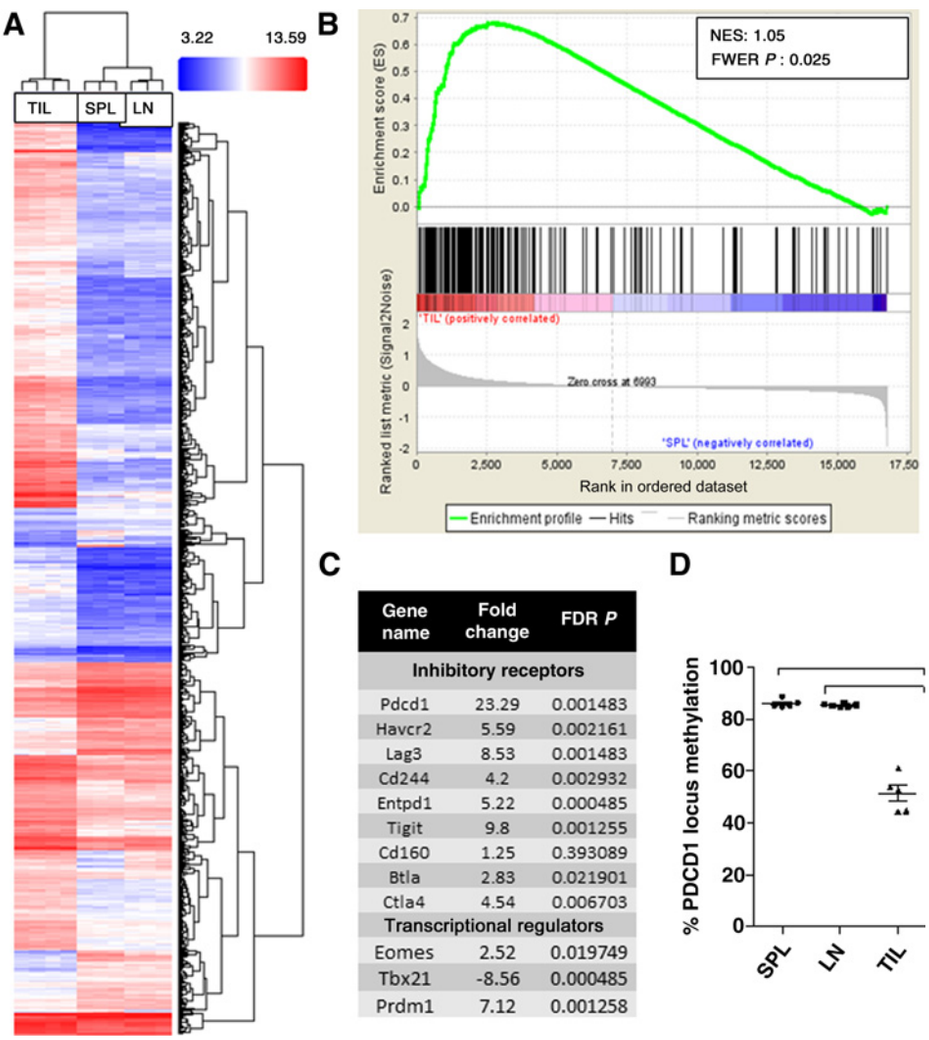

Gene name	Fold change	FDR *P*
Inhibitory receptors		
Pdcd1	23.29	0.001483
Havcr2	5.59	0.002161
Lag3	8.53	0.001483
Cd244	4.2	0.002932
Entpd1	5.22	0.000485
Tigit	9.8	0.001255
Cd160	1.25	0.393089
Btla	2.83	0.021901
Ctla4	4.54	0.006703
Transcriptional regulators		
Eomes	2.52	0.019749
Tbx21	-8.56	0.000485
Prdm1	7.12	0.001258

Figure 4.
TILs demonstrate molecular signatures and epigenetic profiles consistent with T-cell exhaustion. **A,** A hierarchical cluster of gene expression of $CD8^+$ T cells isolated from tumors (TILs), spleens (SPL), or TD cervical LNs. Microarray analysis was performed using the Affymetrix Clariom S Array Platform, and clustering was performed on the 1,071 genes, which were screened from 22,701 total. Comparisons were made via ANOVA; *P* value <0.001 and FDR *P* value < 0.001 (all conditions). **B,** Gene set enrichment analysis (GSEA) was performed with the software GSEA v2.2.3 downloaded from the Broad Institute. Gene sets assessed included GSE30962, publically available through the NCBI on Gene Expression Omnibus. NES, normalized enrichment score. **C,** Table demonstrating representative transcripts over- or underrepresented in TILs compared with SPL. **D,** Analysis of methylation at the PD-1 promoter (Pdcd1) in $CD8^+$ T cells from TILs, SPL, or LNs via ANOVA with repeated measures followed by Bonferroni posttest. ***, $P < 0.0001$.

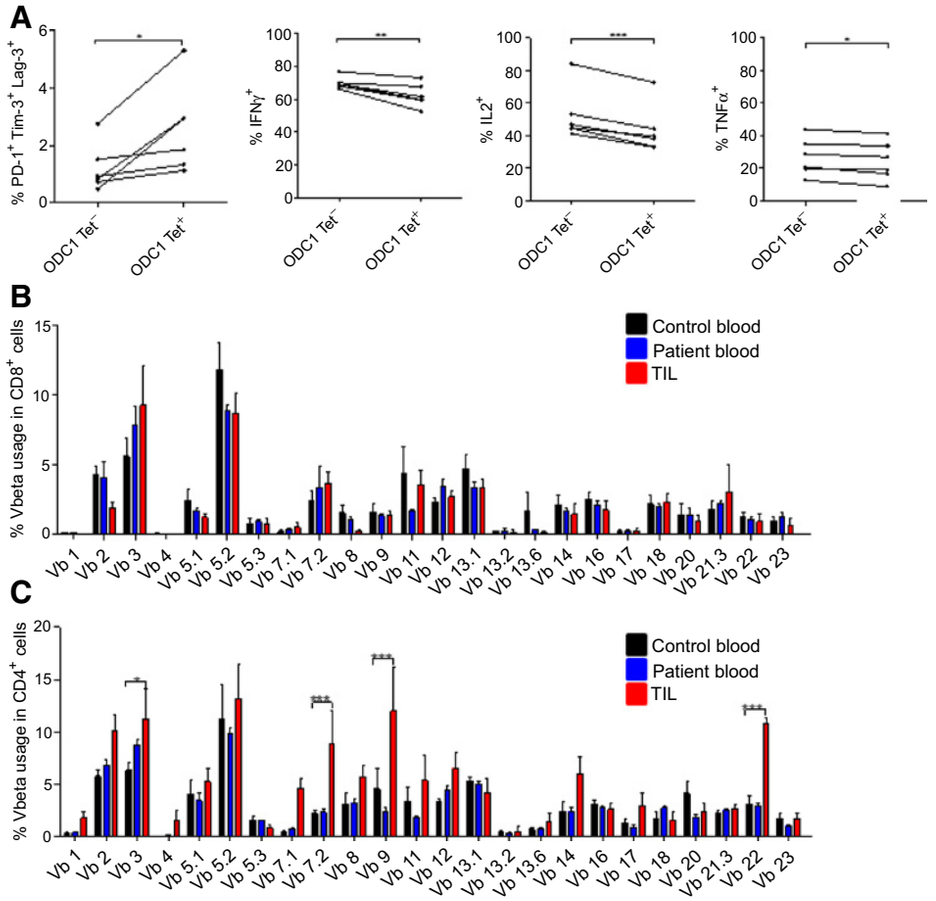

Figure 5.

T-cell exhaustion arises preferentially among tumor-specific T cells. **A,** Five mice were implanted with SMA-560 tumors i.c. Tumors were harvested when mice were moribund and TILs isolated. TILs were stimulated with the ODC-1 peptide for 6 hours, stained with the ODC-1 tetramer conjugated to APC, several immune checkpoints and intracellular stain for cytokines was performed. Significance was assessed via paired *t* test between tetramer-positive and -negative cells. Vbeta analysis was performed on $CD8^+$ (**B**) and $CD4^+$ (**C**) T cells isolated from human GBM TILs ($n = 5$), patient blood ($n = 5$), or control blood ($n = 5$). Significance was assessed using a two-way ANOVA to assess for interaction between Vb and sample type, followed by Bonferroni posttests between patient and control samples. *, $P < 0.05$; **, $P < 0.01$; and ***, $P < 0.001$.

immunogenic endogenous neoantigen (21). As such, we were able to detect neoantigen-specific T cells within IC SMA-560 gliomas using a newly developed ODC1 tetramer. In so doing, we found that ODC1 tetramer–positive T cells contained higher proportions of triply positive $PD\text{-}1^+Tim\text{-}3^+Lag\text{-}3^+$ T cells, and were less functional upon stimulation than their tetramer-negative counterparts (Fig. 5A).

We next sought to determine whether T-cell exhaustion likewise preferentially arises in tumor-specific T cells in human GBM. Given the inability to reliably detect and compare neoantigen-specific T cells across heterogeneous patient specimens, we assessed T-cell clonal expansion as a surrogate measure for antigen specificity, with the goal of phenotypically characterizing any expanded clones. We analyzed the T-cell receptor (TCR) Vβ chains of five matched patient TILs and PBMC samples, and five control PBMC samples. Surprisingly, human GBM-infiltrating $CD8^+$ T cells exhibited no detectable clonal expansion, precluding phenotypic characterization of expanded antigen-specific clones (Fig. 5B). This lack of clonal expansion suggests either ineffectual tumor antigen presentation or the onset of functional defects amid antigen-specific $CD8^+$ T cells immediately upon tumor infiltration. The latter possibility appears more likely, as the limited expansion of $CD8^+$ T cells contrasted starkly with ample clonal expansion amid infiltrating $CD4^+$ T cells (Fig. 5C). Furthermore, we demonstrated that although $CD4^+$ T cells express multiple immune checkpoints (Supplementary Fig. S5A), they remain functional, producing equal amounts of IFNγ as patient and control blood when stimulated (Supplementary Fig. S5B).

T-cell exhaustion signatures reflect tumor type rather than location and are particularly severe among malignant glioma

In prior experiments (Fig. 2A and B), we revealed that the SMA-560 and CT2A glioma models yield consistent yet characteristically distinct exhaustion signatures among infiltrating T cells. This suggested that varying tumor types might elicit reproducibly distinct patterns of exhaustion. To determine whether the i.c. environment might also contribute to the glioma-induced T-cell exhaustion signatures observed, we implanted CT2A and SMA-560 gliomas both IC and s.c. and analyzed TILs at late stages of tumor growth. The phenotypic T-cell exhaustion signature remained constant for each glioma model, independent of the tumor's location in the brain versus the flank (Fig. 6A).

We then determined whether infiltrating T-cell exhaustion signatures differ substantially across gliomas or other solid tumors commonly metastatic to the brain. To this end, we first validated IC engraftment of melanoma (B16F10), breast (E0771), and lung (LLC) carcinoma cell lines (Supplementary Fig. S6A). Subsequently, we implanted B16F10, E0771, and LLC either IC or SQ into syngeneic C57BL/6 mice, harvested tumors when mice were moribund, and determined the TIL exhaustion patterns. Once again, each tumor yielded a characteristic and distinct TIL exhaustion signature that did not vary with i.c. versus peripheral

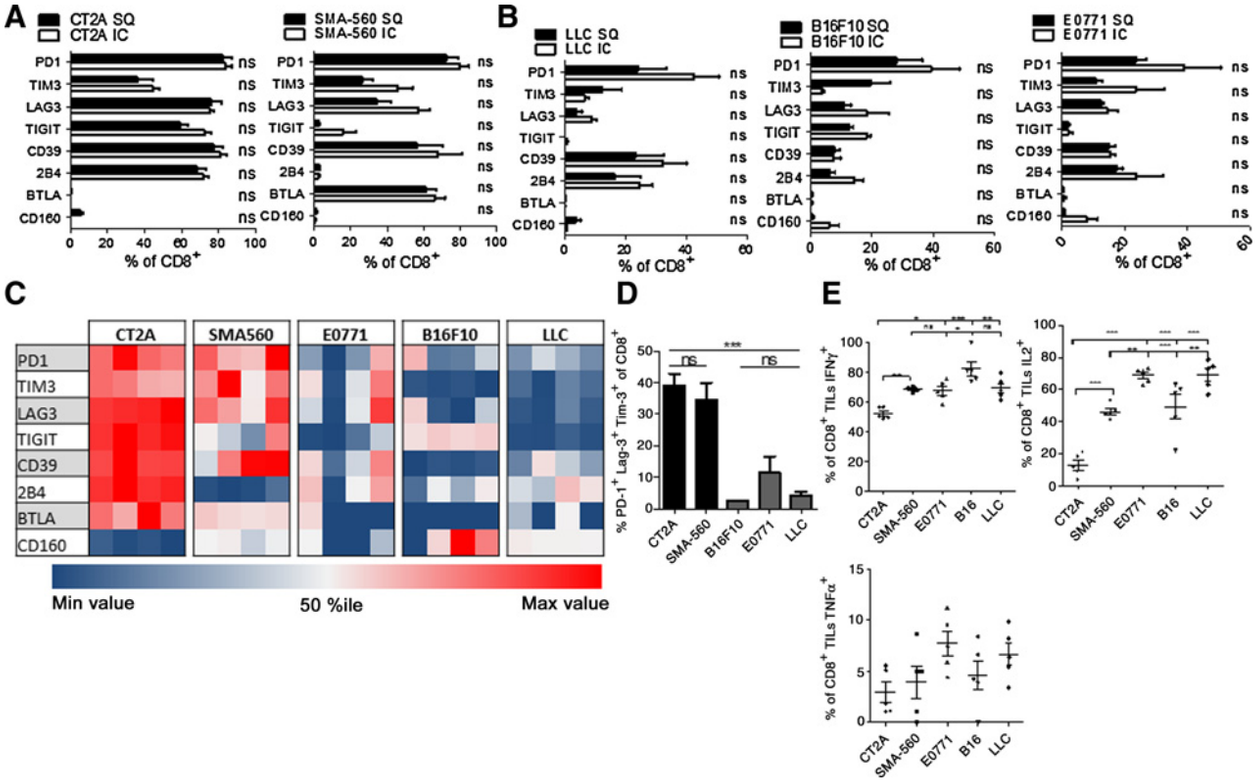

Figure 6.

T-cell exhaustion signatures reflect tumor histology rather than i.c. location and are particularly severe among malignant glioma. **A,** The percentage of CD8$^+$ T cells expressing immune checkpoints within either i.c. or s.c. CT2A and SMA-560 glioma models. TILs were isolated when mice bearing i.c. tumors ($n = 5$) were moribund or when s.c. tumors ($n = 5$) reached 20 mm at the largest diameter. **B,** The percentage of CD8$^+$ T cells expressing various immune checkpoints among i.c. or s.c. B16F10 (melanoma), E0771 (breast), and LLC (lung). **C,** Heat map representing the % of CD8$^+$ TILs expressing immune checkpoints across five different models of i.c. malignancies ($n = 4$). Each row represents one immune checkpoint with associated percentiles. Each column represents an individual mouse. **D,** The percentage of CD8$^+$ TILs coexpressing PD-1, Tim-3, and Lag-3 across five different models of i.c. malignancies. Differences were assessed via one-way ANOVA with Tukey *post hoc* test. **E,** The percentage of CD8$^+$ TIL staining for IFNγ, IL2, and TNFα. *, $P < 0.05$; **, $P < 0.01$; and ***, $P < 0.0001$.

location (Fig. 6B). Representative staining of PD-1 across tumor models is shown in Supplementary Fig. S6B.

Among tumor types, the SMA-560 and CT2A malignant gliomas each yielded TILs with comparatively severe phenotypic exhaustion patterns (Fig. 6C). This included significantly increased numbers of TILs that were triply PD-1$^+$Tim-3$^+$Lag-3$^+$ (Fig. 6D). Correspondingly, TILs isolated from gliomas exhibited the poorest function, with fewer cells producing IL2 than TILs isolated from nonglioma tumor models (Fig. 6E; MFI data shown in Supplementary Fig. S6C). CT2A gliomas, in particular, harbored the least functional T cells, exhibiting significantly impaired IFNγ and IL2 production compared with TILs from SMA-560 gliomas or other tumor models (Fig. 6E). Likewise, the greater functional impairment corresponded to higher levels of the alternative immune checkpoints TIGIT, CD39, and 2B4 on T cells, compared with those of the SMA-560 glioma model (Fig. 6C). Importantly, the severity of TIL exhaustion patterns did not appear to correspond to levels of T-cell infiltration across tumor types: CT2A and LLC, despite very different exhaustion signatures, both demonstrated low T-cell infiltration ("cold" tumors), whereas E0771, SMA-560, and E0771 all demonstrated greater degrees of infiltration (Supplementary Fig. S7). The degree of T-cell infiltration may not influence T-cell exhaustion profiles, suggesting that the association of T-cell infiltration to treatment response to checkpoint blockade may not be associated with degree of T-cell exhaustion (29). Taken together, these findings suggest that exhaustion patterns among tumor-infiltrating T cells are (1) determined by tumor-intrinsic factors and not environment; (2) strongly influence infiltrating T-cell function; and (3) vary in severity across and reflect tumor type, with gliomas instigating particularly severe exhaustion.

Discussion

Immune checkpoint blockade has garnered significant interest in recent years following dramatic successes against a variety of solid tumors (30–34) and resultant FDA approval as an immunotherapeutic strategy for multiple malignancies. The efficacy of classical checkpoint blockade (specifically anti–PD-1 and anti–CTLA-4) may be hindered, however, by the emergence of a number of secondary or alternative checkpoints on T cells (18), including TIM-3, LAG-3, BTLA, 2B4, CD160, CD39, and TIGIT (35–37). Mounting expression of these alternative checkpoints on T cells provides additional avenues for T-cell shutdown following

activation, but also serves to signal T-cell transition into a dysfunctional, exhausted state (37, 38). Such exhaustion may be reversible in earlier stages, but can rapidly progress to a late phase in which function declines beyond rescue (39, 40).

T-cell dysfunction has long been a hallmark of GBM, as we, and others, have highlighted (4–6). Classically, such dysfunction can be categorized under the labels of senescence, ignorance, anergy, tolerance, and exhaustion (41). Anergy and tolerance are well characterized in GBM, but this study suggests exhaustion as a major contributor to the failure of T cells that otherwise successfully arrive at tumor and initially become activated. Whereas much focus to date has been on activating T cells and ensuring their access to tumors situated within the confines of the brain, we demonstrate that those T cells successfully arriving tumor are still rendered hyporesponsive by the tumor, with exhaustion revealed as a predominant and underappreciated mode of dysfunction. Accordingly, we are among the first to thoroughly characterize immune checkpoint expression on GBM patient $CD8^+$ TILs, and to subsequently credential such expression as *bona fide* exhaustion by performing functional and transcriptome analyses. Our study highlights that phenotypic expression of checkpoints may not accurately reflect an exhausted state: we show that $CD4^+$ TILs remain functional despite expression of multiple immune checkpoints, and that $CD8^+$ T cells expressing PD-1 alone remain functional. In light of these findings, we demonstrate that T-cell functional status and molecular signatures remain important confirmations of true T-cell exhaustion.

Prevalent among TILs in both patients and mice with GBM are T cells coexpressing PD-1 in conjunction with the alternative inhibitory immune checkpoints, TIM-3 and LAG-3. This coexpression appears to specifically mark TILs as hypofunctional in our study and suggests the importance of TIM-3 and LAG-3 as immune checkpoint targets of import in GBM. Preclinical work has indeed highlighted a possible synergy between PD-1, Tim-3, and Lag-3 blockade in mice with GBM (42). Monoclonal antibodies blocking human TIM-3 and LAG-3 are in early phase clinical trials in GBM and other solid tumors. A phase I clinical trial of anti–LAG-3 alone or in combination with anti–PD-1 is currently recruiting GBM patients (NCT02658981), whereas a phase I clinical trial of anti–TIM-3 alone or in combination with anti–PD-1 is currently recruiting patients with advanced solid tumors (NCT02817633). The results of these trials will help to assess whether combinatorial checkpoint blockade in GBM might increase the likelihood of functional rescue for T cells infiltrating these tumors. Data from these trials will be highly anticipated, given the recent announcements regarding the failure of PD-1 blockade monotherapy in a phase III trial in GBM.

Checkpoint blockade, as with all immunotherapies, encounters multiple challenges in GBM, including considerable intratumoral heterogeneity (2, 43, 44), poor immunogenicity (45, 46), low mutational burden (47), poor T-cell infiltration (48), and substantial tumor-elicited T-cell dysfunction (10). Each of these challenges may need to be addressed before we can anticipate the ingress of prodigious immunotherapeutic success in GBM. GBM has frequently posed more difficulty than other cancers, evident in what remains a 100% mortality rate, despite what is essentially a local disease with only exceedingly rare cases of metastasis. Yet, despite its exclusively local progression, GBM elicits severe immune dysfunction, both locally and systemically. Here, we demonstrate that GBM also elicits a uniquely severe T-cell exhaustion signature compared with other tumor types. This finding is manifested in the increased expression of multiple coinhibitory immune checkpoints and the decreased functional capacity of glioma-infiltrating T cells in comparison with other T cells infiltrating other models of i.c. malignancy. The mounting expression of alternative immune checkpoints may indicate a state of terminal exhaustion that cannot be reversed by traditional checkpoint blockade alone.

Importantly, different tumor histologies (and even different glioma models) in our studies elicited differing exhaustion signatures among infiltrating T cells, regardless of where in the body these tumors were introduced. These results suggest that different tumors might induce reproducibly distinct patterns of exhaustion. They also therefore suggest that the mechanisms whereby tumors induce exhaustion among T cells may not be universal and may represent a "convergent evolution" of sorts. These findings, however, may also begin to provide the foundation for personalized and rationally designed alternative immune checkpoint blockade: checkpoint blockade strategies successful in one cancer type may not be appropriate in others, and may ultimately require thorough characterization of the dysfunction elicited among a given patient's TILs.

Lastly, the lack of influence of tumor location on TIL exhaustion signature suggests a limited role for central nervous system (CNS)-specific factors in the programming of the T-cell exhaustion, a point of optimism for those looking to thwart T-cell exhaustion within the brain. Such strategies, as applied to primary peripheral tumors metastasizing to the brain, may prove equally successful against brain metastases or primary brain tumors, once afforded appropriate CNS access. Future studies will need to examine factors influencing tumor-specific induction of T-cell exhaustion, as well as the capacities for T-cell rescue with rationally designed immune checkpoint blockade or additional strategies.

Disclosure of Potential Conflicts of Interest

G. Dranoff is an employee of Novartis. G.P. Dunn holds ownership interest (including patents) in Immunovalent Therapeutics. No potential conflicts of interest were disclosed by the other authors.

Authors' Contributions

Conception and design: K. Woroniecka, P. Chongsathidkiet, S.H. Farber, C. Jackson, G.P. Dunn, P.E. Fecci

Development of methodology: K. Woroniecka, P. Chongsathidkiet, C. Jackson, L.J. Hansen, Y.-R.A. Yu, D.D. Bigner, K.J. Weinhold, G.P. Dunn, P.E. Fecci

Acquisition of data (provided animals, acquired and managed patients, provided facilities, etc.): K. Woroniecka, P. Chongsathidkiet, K. Rhodin, H. Kemeny, C. Dechant, S.H. Farber, A.A. Elsamadicy, X. Cui, C. Jackson, L.J. Hansen, V. Chandramohan, D.D. Bigner, P.E. Fecci

Analysis and interpretation of data (e.g., statistical analysis, biostatistics, computational analysis): K. Woroniecka, P. Chongsathidkiet, S.H. Farber, L. Sanchez-Perez, A. Giles, P. Healy, G.P. Dunn, P.E. Fecci

Writing, review, and/or revision of the manuscript: K. Woroniecka, P. Chongsathidkiet, S.H. Farber, A.A. Elsamadicy, S. Koyama, C. Jackson, T.M. Johanns, D.D. Bigner, A. Giles, P. Healy, G. Dranoff, K.J. Weinhold, P.E. Fecci

Administrative, technical, or material support (i.e., reporting or organizing data, constructing databases): K. Woroniecka, X. Cui, T.M. Johanns, D.D. Bigner, P.E. Fecci

Study supervision: L. Sanchez-Perez, P.E. Fecci

Acknowledgments

The work was supported in part by the National Institutes of Health Duke Brain SPORE Developmental Research Program (P.E. Fecci), the Medical Scientist Training Program at Duke University School of Medicine (K. Woroniecka), the NIH grant K08NS092912 (G.P. Dunn), the American

Cancer Society-Institutional Research grant (G.P. Dunn), and the Physician-Scientist Training Program at Washington University School of Medicine (T.M. Johanns).

The costs of publication of this article were defrayed in part by the payment of page charges. This article must therefore be hereby marked *advertisement* in accordance with 18 U.S.C. Section 1734 solely to indicate this fact.

Received June 28, 2017; revised January 2, 2018; accepted February 1, 2018; published first February 7, 2018.

References

1. Stupp R, Hegi ME, Mason WP, van den Bent MJ, Taphoorn MJ, Janzer RC, et al. Effects of radiotherapy with concomitant and adjuvant temozolomide versus radiotherapy alone on survival in glioblastoma in a randomised phase III study: 5-year analysis of the EORTC-NCIC trial. Lancet Oncol 2009;10:459–66.
2. Patel AP, Tirosh I, Trombetta JJ, Shalek AK, Gillespie SM, Wakimoto H, et al. Single-cell RNA-seq highlights intratumoral heterogeneity in primary glioblastoma. Science 2014;344:1396–401.
3. Kmiecik J, Poli A, Brons NH, Waha A, Eide GE, Enger PO, et al. Elevated CD3+ and CD8+ tumor-infiltrating immune cells correlate with prolonged survival in glioblastoma patients despite integrated immunosuppressive mechanisms in the tumor microenvironment and at the systemic level. J Neuroimmunol 2013;264:71–83.
4. Dix AR, Brooks WH, Roszman TL, Morford LA. Immune defects observed in patients with primary malignant brain tumors. J Neuroimmunol 1999; 100:216–32.
5. Dunn GP, Fecci PE, Curry WT. Cancer immunoediting in malignant glioma. Neurosurgery 2012;71:201–22; discussion 22–3.
6. Fecci PE, Heimberger AB, Sampson JH. Immunotherapy for primary brain tumors: no longer a matter of privilege. Clin Cancer Res 2014; 20:5620–9.
7. Brooks WH, Roszman TL, Mahaley MS, Woosley RE. Immunobiology of primary intracranial tumours. II. Analysis of lymphocyte subpopulations in patients with primary brain tumours. Clin Exp Immunol 1977;29:61–6.
8. Elliott LH, Brooks WH, Roszman TL. Cytokinetic basis for the impaired activation of lymphocytes from patients with primary intracranial tumors. J Immunol 1984;132:1208–15.
9. Ausiello CM, Palma C, Maleci A, Spagnoli GC, Amici C, Antonelli G, et al. Cell mediated cytotoxicity and cytokine production in peripheral blood mononuclear cells of glioma patients. Eur J Cancer 1991;27: 646–50.
10. Fecci PE, Mitchell DA, Whitesides JF, Xie W, Friedman AH, Archer GE, et al. Increased regulatory T-cell fraction amidst a diminished CD4 compartment explains cellular immune defects in patients with malignant glioma. Cancer Res 2006;66:3294–302.
11. El Andaloussi A, Lesniak MS. An increase in CD4+CD25+FOXP3+ regulatory T cells in tumor-infiltrating lymphocytes of human glioblastoma multiforme. Neuro-oncol 2006;8:234–43.
12. El Andaloussi A, Han Y, Lesniak MS. Prolongation of survival following depletion of CD4+CD25+ regulatory T cells in mice with experimental brain tumors. J Neurosurg 2006;105:430–7.
13. Fecci PE, Sweeney AE, Grossi PM, Nair SK, Learn CA, Mitchell DA, et al. Systemic anti-CD25 monoclonal antibody administration safely enhances immunity in murine glioma without eliminating regulatory T cells. Clin Cancer Res 2006;12(14 Pt 1):4294–305.
14. Wherry EJ, Blattman JN, Murali-Krishna K, van der Most R, Ahmed R. Viral persistence alters CD8 T-cell immunodominance and tissue distribution and results in distinct stages of functional impairment. J Virol 2003;77: 4911–27.
15. Zajac AJ, Blattman JN, Murali-Krishna K, Sourdive DJ, Suresh M, Altman JD, et al. Viral immune evasion due to persistence of activated T cells without effector function. J Exp Med 1998;188:2205–13.
16. Lee PP, Yee C, Savage PA, Fong L, Brockstedt D, Weber JS, et al. Characterization of circulating T cells specific for tumor-associated antigens in melanoma patients. Nat Med 1999;5:677–85.
17. Wherry EJ, Ha SJ, Kaech SM, Haining WN, Sarkar S, Kalia V, et al. Molecular signature of CD8+ T cell exhaustion during chronic viral infection. Immunity 2007;27:670–84.
18. Koyama S, Akbay EA, Li YY, Herter-Sprie GS, Buczkowski KA, Richards WG, et al. Adaptive resistance to therapeutic PD-1 blockade is associated with upregulation of alternative immune checkpoints. Nat Commun 2016; 7:10501.
19. Serano RD, Pegram CN, Bigner DD. Tumorigenic cell culture lines from a spontaneous VM/Dk murine astrocytoma (SMA). Acta Neuropathol 1980;51:53–64.
20. Martinez-Murillo R, Martinez A. Standardization of an orthotopic mouse brain tumor model following transplantation of CT-2A astrocytoma cells. Histol Histopathol 2007;22:1309–26.
21. Johanns TM, Ward JP, Miller CA, Wilson C, Kobayashi DK, Bender D, et al. Endogenous neoantigen-specific CD8 T cells identified in two glioblastoma models using a cancer immunogenomics approach. Cancer Immunol Res 2016;4:1007–15.
22. McPherson RC, Konkel JE, Prendergast CT, Thomson JP, Ottaviano R, Leech MD, et al. Epigenetic modification of the PD-1 (Pdcd1) promoter in effector CD4(+) T cells tolerized by peptide immunotherapy. Elife 2014;3.
23. Baitsch L, Baumgaertner P, Devevre E, Raghav SK, Legat A, Barba L, et al. Exhaustion of tumor-specific CD8(+) T cells in metastases from melanoma patients. J Clin Invest 2011;121:2350–60.
24. Derre L, Rivals JP, Jandus C, Pastor S, Rimoldi D, Romero P, et al. BTLA mediates inhibition of human tumor-specific CD8+ T cells that can be partially reversed by vaccination. J Clin Invest 2010;120:157–67.
25. West EE, Youngblood B, Tan WG, Jin HT, Araki K, Alexe G, et al. Tight regulation of memory CD8(+) T cells limits their effectiveness during sustained high viral load. Immunity 2011;35:285–98.
26. Paley MA, Kroy DC, Odorizzi PM, Johnnidis JB, Dolfi DV, Barnett BE, et al. Progenitor and terminal subsets of CD8+ T cells cooperate to contain chronic viral infection. Science 2012;338:1220–5.
27. Shin H, Blackburn SD, Intlekofer AM, Kao C, Angelosanto JM, Reiner SL, et al. A role for the transcriptional repressor Blimp-1 in CD8(+) T cell exhaustion during chronic viral infection. Immunity 2009;31:309–20.
28. Youngblood B, Oestreich KJ, Ha SJ, Duraiswamy J, Akondy RS, West EE, et al. Chronic virus infection enforces demethylation of the locus that encodes PD-1 in antigen-specific CD8(+) T cells. Immunity 2011; 35:400–12.
29. Tang H, Wang Y, Chlewicki LK, Zhang Y, Guo J, Liang W, et al. Facilitating T cell infiltration in tumor microenvironment overcomes resistance to PD-L1 blockade. Cancer Cell 2016;30:500.
30. Larkin J, Hodi FS, Wolchok JD. Combined nivolumab and ipilimumab or monotherapy in untreated melanoma. N Engl J Med 2015;373:1270–1.
31. Robert C, Schachter J, Long GV, Arance A, Grob JJ, Mortier L, et al. Pembrolizumab versus ipilimumab in advanced melanoma. N Engl J Med 2015;372:2521–32.
32. Motzer RJ, Escudier B, McDermott DF, George S, Hammers HJ, Srinivas S, et al. Nivolumab versus everolimus in advanced renal-cell carcinoma. N Engl J Med 2015;373:1803–13.
33. Garon EB, Rizvi NA, Hui R, Leighl N, Balmanoukian AS, Eder JP, et al. Pembrolizumab for the treatment of non-small-cell lung cancer. N Engl J Med 2015;372:2018–28.
34. Ferris RL, Blumenschein G Jr, Fayette J, Guigay J, Colevas AD, Licitra L, et al. Nivolumab for recurrent squamous-cell carcinoma of the head and neck. N Engl J Med 2016;375:1856–67.
35. Chauvin JM, Pagliano O, Fourcade J, Sun Z, Wang H, Sander C, et al. TIGIT and PD-1 impair tumor antigen-specific CD8(+) T cells in melanoma patients. J Clin Invest 2015;125:2046–58.
36. Blackburn SD, Shin H, Haining WN, Zou T, Workman CJ, Polley A, et al. Coregulation of CD8+ T cell exhaustion by multiple inhibitory receptors during chronic viral infection. Nat Immunol 2009;10:29–37.
37. Woo SR, Turnis ME, Goldberg MV, Bankoti J, Selby M, Nirschl CJ, et al. Immune inhibitory molecules LAG-3 and PD-1 synergistically regulate T-cell function to promote tumoral immune escape. Cancer Res 2012;72: 917–27.

38. Kurtulus S, Sakuishi K, Ngiow SF, Joller N, Tan DJ, Teng MW, et al. TIGIT predominantly regulates the immune response via regulatory T cells. J Clin Invest 2015;125:4053–62.
39. Angelosanto JM, Blackburn SD, Crawford A, Wherry EJ. Progressive loss of memory T cell potential and commitment to exhaustion during chronic viral infection. J Virol 2012;86:8161–70.
40. Wherry EJ, Kurachi M. Molecular and cellular insights into T cell exhaustion. Nat Rev Immunol 2015;15:486–99.
41. Mirzaei R, Sarkar S, Yong VW. T cell exhaustion in glioblastoma: intricacies of immune checkpoints. Trends Immunol 2017;38:104–15.
42. Kim JE, Patel MA, Mangraviti A, Kim ES, Theodros D, Velarde E, et al. Combination therapy with anti-PD-1, anti-TIM-3, and focal radiation results in regression of murine gliomas. Clin Cancer Res 2017;23:124–36.
43. Meyer M, Reimand J, Lan X, Head R, Zhu X, Kushida M, et al. Single cell-derived clonal analysis of human glioblastoma links functional and genomic heterogeneity. Proc Natl Acad Sci U S A 2015;112:851–6.
44. Soeda A, Hara A, Kunisada T, Yoshimura S, Iwama T, Park DM. The evidence of glioblastoma heterogeneity. Sci Rep 2015;5:7979.
45. Zagzag D, Salnikow K, Chiriboga L, Yee H, Lan L, Ali MA, et al. Downregulation of major histocompatibility complex antigens in invading glioma cells: stealth invasion of the brain. Lab Invest 2005;85:328–41.
46. Yeung JT, Hamilton RL, Ohnishi K, Ikeura M, Potter DM, Nikiforova MN, et al. LOH in the HLA class I region at 6p21 is associated with shorter survival in newly diagnosed adult glioblastoma. Clin Cancer Res 2013;19:1816–26.
47. Parsons DW, Jones S, Zhang X, Lin JC, Leary RJ, Angenendt P, et al. An integrated genomic analysis of human glioblastoma multiforme. Science 2008;321:1807–12.
48. Lohr J, Ratliff T, Huppertz A, Ge Y, Dictus C, Ahmadi R, et al. Effector T-cell infiltration positively impacts survival of glioblastoma patients and is impaired by tumor-derived TGF-beta. Clin Cancer Res 2011;17:4296–308.